Electronic Supplementary Material (ESI) for Journal of Materials Chemistry A.

Supporting Information

Partially Delocalized Charge in Fe-doped $NiCo_2S_4$ Nanosheet-Mesoporous Carbon-Composites for High-Voltage Supercapacitors

Feili Lai, Jianrui Feng, Tobias Heil, Zhihong Tian, Johannes Schmidt, Gui-Chang Wang, and Martin Oschatz

Synthesis of SBA-15. SBA-15 hard template was synthesized as reported by Zhao et al.[1,2] Briefly, 33.4 g triblock copolymer of poly(ethylene glycol)-block-poly(propylene glycol)-block-poly(ethylene glycol) (Pluronic P123, Sigma Aldrich) was dissolved in 623 mL HCl solution with a concentration of 0.33 mol L^{-1}. Then, 71.8 g of tetraethyl orthosilicate (TEOS, Alfa Aesar) was added into the above solution with stirring for 24 h. After hydrothermal reaction at 115 ºC for 6 h, the solid product was filtered, washed with water and ethanol, and dried at 60 ºC overnight. Finally, the dried product was calcined in air for 10 h at 550 ºC to get the white powder of SBA-15 hard template.

Synthesis of CMK-3. The ordered mesoporous carbon CMK-3 was synthesized using highly ordered hexagonal mesoporous silica of SBA-15 as hard template and sucrose as carbon source.[3] Briefly, 1 g of SBA-15 powder was impregnated with sucrose solution containing 1.25 g sucrose, 0.14 g concentrated H_2SO_4, and 5 mL H_2O. The mixture was treated in an oven at 100 ºC for 6 h and then at 160 ºC for another 6 h. For a repeated cycle, the above powder was impregnated with sucrose solution containing 0.8 g sucrose, 0.09 g concentrated H_2SO_4, and 5 mL H_2O. The mixture was treated at 100 ºC for 6 h, and at 160 ºC for another 6 h again. The resulting product which contained partially polymerized carbon precursor and SBA-15 was carbonized at 900ºC for 2 h under N_2 flow. SBA-15 was removed by heating the carbon/silica composite in 4 M NaOH aqueous solution at 115 ºC overnight. Finally, the obtained template-free CMK-3 was filtered, washed with deionized water and ethanol, and dried at 60 ºC overnight.

Synthesis of N,S-CMK-3. The N- and S-doped ordered mesoporous carbon (N,S-

CMK-3) was synthesized based on our previously reported work.[4] Typically, 200 mg of CMK-3 and 400 mg thiourea (CN_2H_4S) were mixed together, and heated at 850 ºC for 3 h with a heating rate of 2 ºC min^{-1} under N_2 atmosphere.

Synthesis of Fe-$NiCo_2S_4$@N,S-CMK-3 and $NiCo_2S_4$@N,S-CMK-3. The Fe-$NiCo_2S_4$@N,S-CMK-3 and $NiCo_2S_4$@N,S-CMK-3 were synthesized by hydrothermal reaction. Firstly, 276.3 mg, 553.1 mg, 19 mg, 304.5 mg, and 120 mg of $Ni(NO_3)_2{\cdot}6H_2O$, $Co(NO_3)_2{\cdot}6H_2O$, Fe_2Cl, thiourea, and urea were firstly dissolved in 30 mL deionized water to form a homogeneous reaction solution. Then, 150 mg of N,S-CMK-3 powder was dispersed into the above solution by sonication for 2 h. After transferring into a Teflon-lined stainless-steel 50 mL autoclave, the mixed solution maintained at 160 ºC for 12 h. The product was collected by centrifugation, washed with deionized water/ethanol, and dried at 60 ºC overnight. Then, the above powder was annealed at 280 ºC for 2 h with a ramp rate of 5 ºC min^{-1} under N_2 atmosphere. For comparison, non-iron-doped $NiCo_2S_4$@N,S-CMK-3 and NiCo2S4 bulk were prepared by using the same steps except for adding the Fe^{2+} salt and N,S-CMK-3 template, respectively.

Characterizations. Morphology of the materials was observed by scanning electron microscopy (SEM, LEO 1550-Gemini) operating at 3 kV, and high-resolution transmission electron microscopy (HRTEM, JEOL ARM 200F) operating at 200 kV. X-ray diffraction (XRD) patterns were recorded on a Smartlab X-ray diffractometer (Cu Kα, λ = 0.1541 nm). N_2 physisorption experiments were carried out at -196 °C with 40-60 mg sample on a Quadrasorb apparatus from Quantachrome Instruments. Prior to all measurements, the samples were outgassed at 150 °C for 20 h under vacuum. Specific surface areas (SSAs) were calculated using the multi-point Brunauer-Emmett-Teller (BET) model (p/p_0 = 0.05-0.2). Total pore volumes (V_t) were determined at p/p_0 = 0.95. Pore size distributions were calculated using the quenched-solid density functional theory (QSDFT) method (adsorption branch kernel) for N_2 adsorbed on carbon with a slit/cylindrical pore shape at -196 °C. X-ray photoelectron spectroscopy (XPS) measurements were performed using a ThermoScientific K-Alpha+ X-ray Photoelectron Spectrometer. All samples were analyzed using a microfocused, monochromated Al K α X-ray source (1486.68 eV; 400 μm spot size).The binding energies obtained in the XPS spectral analysis were corrected for specimen charging by referencing C 1s to 284.8 eV. Thermogravimetric analysis (TGA) was operated with a Netzsch TG 209 F1 device under an artificial air flow with a heating rate of 5 ºC min^{-1}.

Theory calculation. The density functional theory (DFT) calculations were carried out using the Vienna ab initio simulation package (VASP) with the projector augmented wave (PAW)[5] pseudopotentials and the function of Perdew, Burke and Ernzerhof (PBE)[6] based on the generalized gradient approximation (GGA). A cut-off energy of 400 eV was used for the plane-wave basis set. The Brillouin zone was sampled on the basis of the Monkhorst–Pack scheme[7] with a 3 × 3 × 1 k-point mesh. A $4\sqrt{3} \times 6$ graphene supercell with a vacuum region of 15 Å was adopted. The convergence criteria of self-consistent field (SCF) for electronic relaxation and force for atomic relaxation were 1×10^{-5} eV and 0.01 eV Å^{-1}, respectively. The adsorption energy was defined as $E_{ad} = E_{sub+ion} – E_{sub} – E_{ion}$, where $E_{sub+ion}$, E_{sub} and E_{ion} were the total energies of substrates with the electrolyte ions, clean substrates and the isolated electrolyte ions, respectively. Spin polarization were considered in all the calculations.

Electrochemical test. To prepare free-standing electrodes, various composite materials and polytetrafluoroethylene (PTFE, 60 wt% solution in H_2O from Sigma Aldrich) were mixed at a mass ratio of 9:1, to form a uniform suspension using ethanol as the solvent. After the evaporation of ethanol, a rubber-like consistency was formed, placed into aluminum foil, and rolled into thin sheets with a thickness of 180±10 μm by using a commercial roll mill. After dried at 120 °C for 12 h under vacuum, the thin sheets were punched into free-standing electrode disks of 10 mm in diameter, the areal density of which was about 5 mg cm^{-2}. Typically, the symmetric and asymmetric supercapacitors were assembled using a pair of circular electrodes sandwiching a separator (Dreamweaver International Inc., 13 mm in diameter), with 100 μL $EMIMBF_4$ liquid as electrolyte, two platinum foils as current collectors and two electrode disks as working electrodes. All the two electrode supercapacitors were assembled in an argon filled glove box ($H_2O < 0.1$ ppm, $O_2 < 0.1$ ppm). A Biologic MPG-2 galvanostat/potentiostat was applied for electrochemical characterization. The electrochemical impedance spectroscopy was performed at open circuit potential with a sinusoidal signal over a frequency range from 20 kHz to 10^{-2} Hz at an amplitude of 10 mV. Cyclic voltammetry (CV) tests were performed at a scan rate from 2 to 200 mV s^{-1}, from which the specific capacitance of the electrode materials can be calculated as the following equation:

$$C = \frac{2\int IdV}{v \times m \times V} \qquad (1)$$

Where I is the current, V is the potential, v is the scan rate, and m is the mass of the electroactive materials on one electrode.

Galvanostatic charge-discharge (GCD) tests were performed under different current densities from 0.1 to 20 A g^{-1}, from which the specific capacitance of the as assembled device can also be calculated as the following equation:

$$C = \frac{I \times \Delta t}{2mV} \qquad (2)$$

Where I is the constant current in discharging, Δt is the discharge time, m is the average mass for the positive and negative electrodes, and V is the voltage change during discharge (excluding the IR drop).

The energy density (Wh kg^{-1}) and power density (W kg^{-1}) of the symmetric supercapacitors were evaluated from the following equations:

$$E = \frac{1}{2} \times C \times V^2 \qquad (3)$$

$$P = \frac{E}{\Delta t} \qquad (4)$$

Where C is the cell specific capacitance, V is the voltage change during discharge, and

Δt is the discharge time.

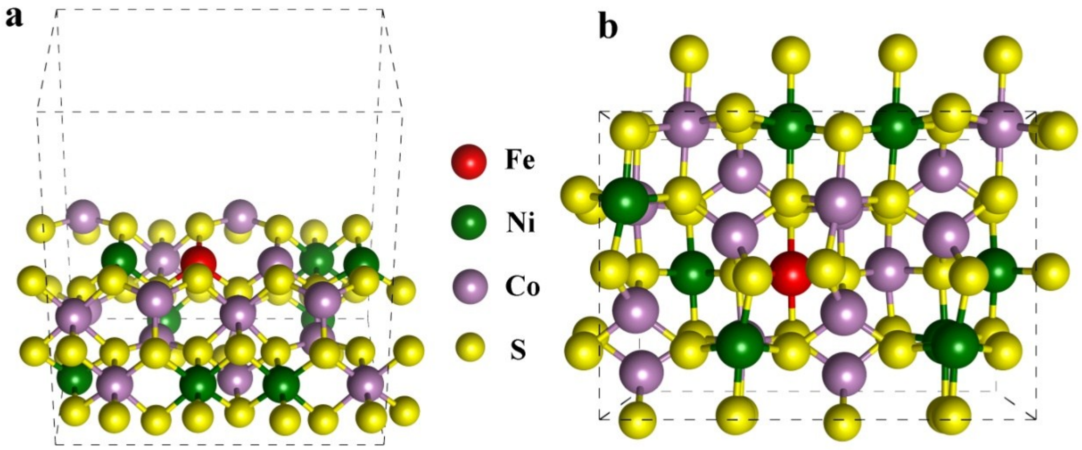

Figure S1. (a) Calculated structure of iron-doped $NiCo_2S_4$ (a=9.424, b=13.328, c=15.078 Å); (b) view from z axis.

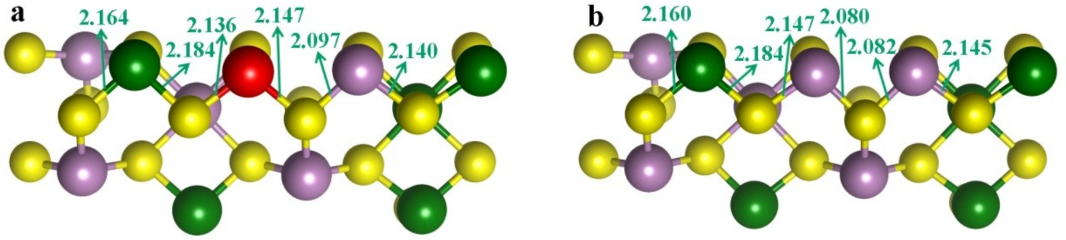

Figure S2. Optimized crystal structures for (a) iron-doped $NiCo_2S_4$, and (b) $NiCo_2S_4$. Bonds length are in Å.

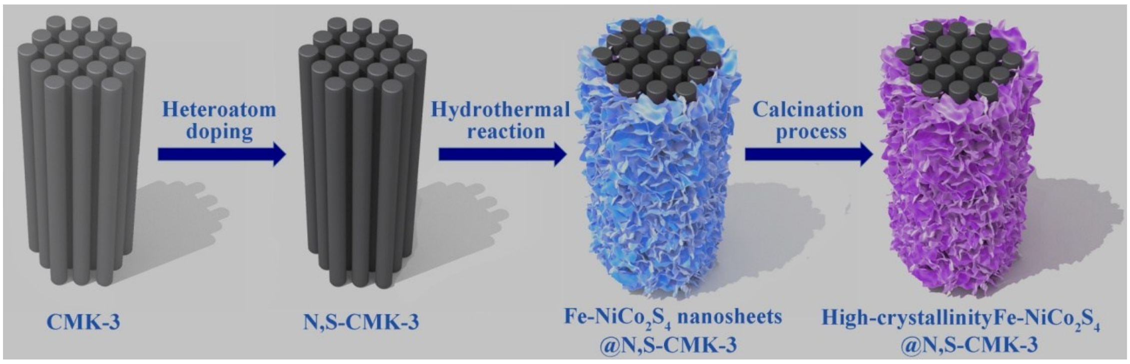

Figure S3. Synthesis process of the Fe-NiCo$_2$S$_4$@N,S-CMK-3 composite.

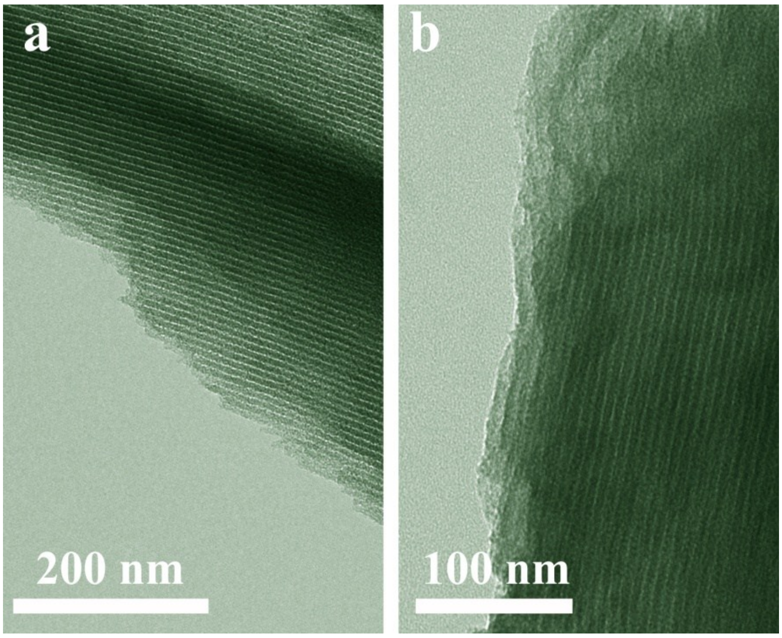

Figure S4. TEM images of (a) ordered mesoporous carbon (CMK-3), and (b) N,S-doped ordered mesoporous carbon (N,S-CMK-3).

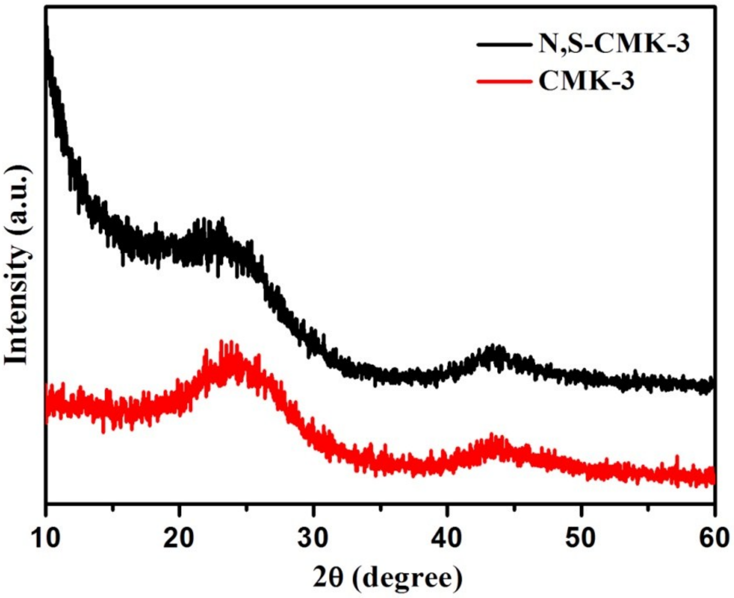

Figure S5. XRD patterns of CMK-3 and N,S-CMK-3.

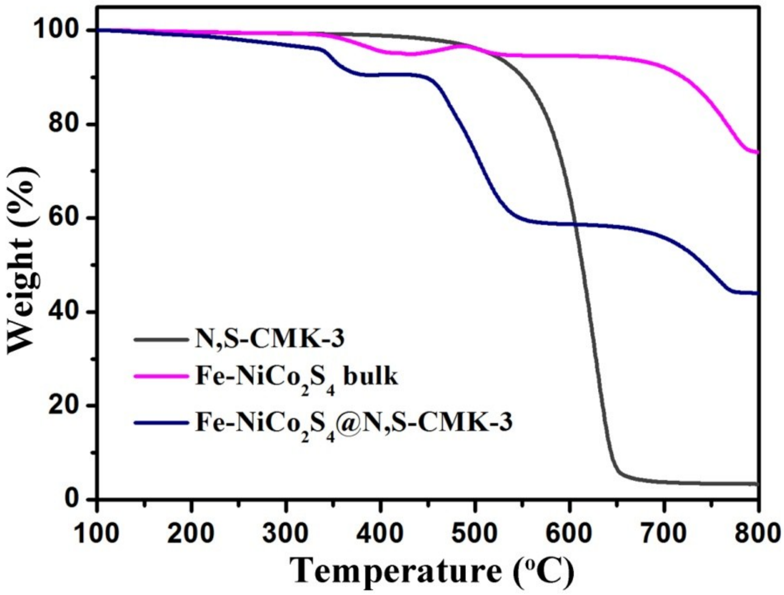

Figure S6. TGA profiles of N,S-CMK-3, Fe-NiCo$_2$S$_4$ bulk, and Fe-NiCo$_2$S$_4$@N,S-CMK-3 under air flow with a heating rate of 5 ºC min^{-1}.

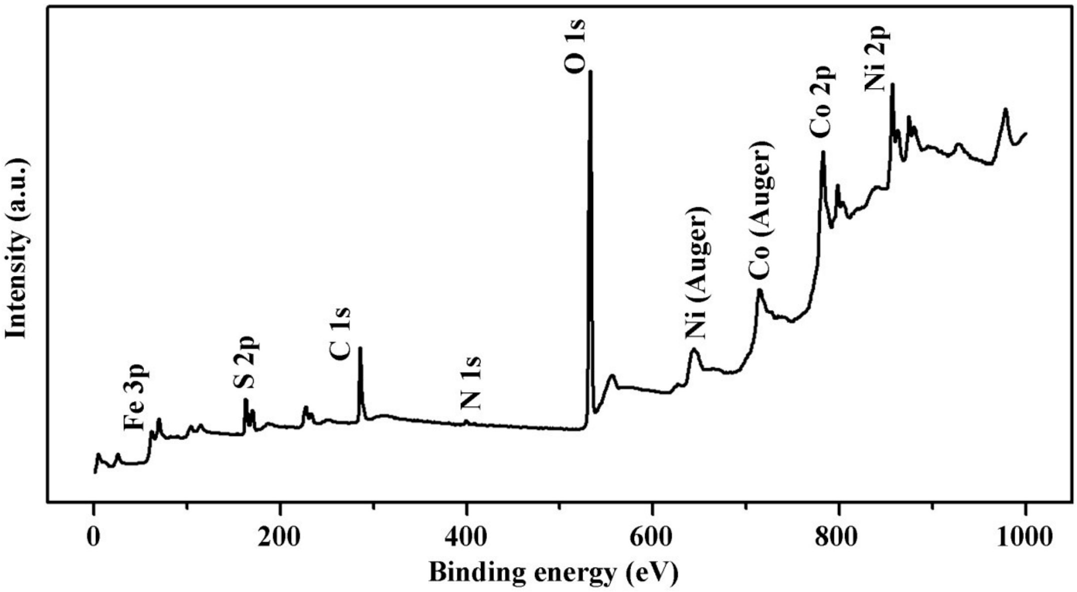

Figure S7.XPS survey spectrum of Fe-$NiCo_2S_4$@N,S-CMK-3.

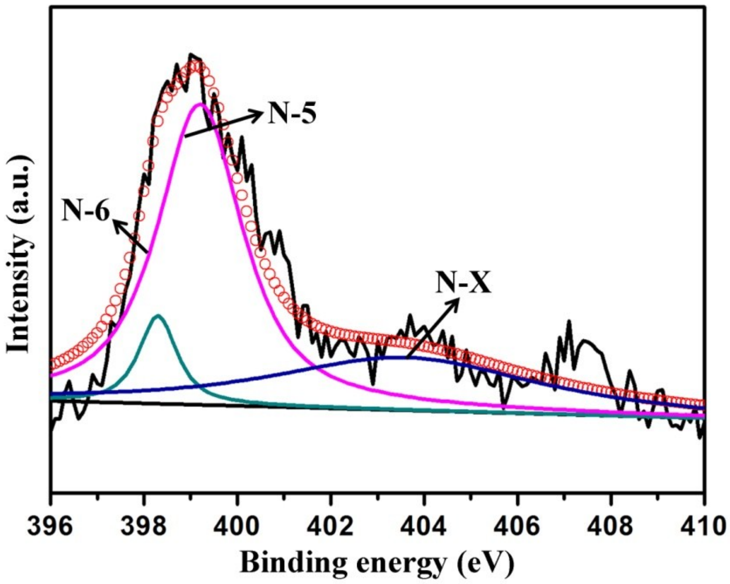

Figure S8. High resolution spectrum and fitting curves of the N 1s peak of Fe-$NiCo_2S_4$@N,S-CMK-3.

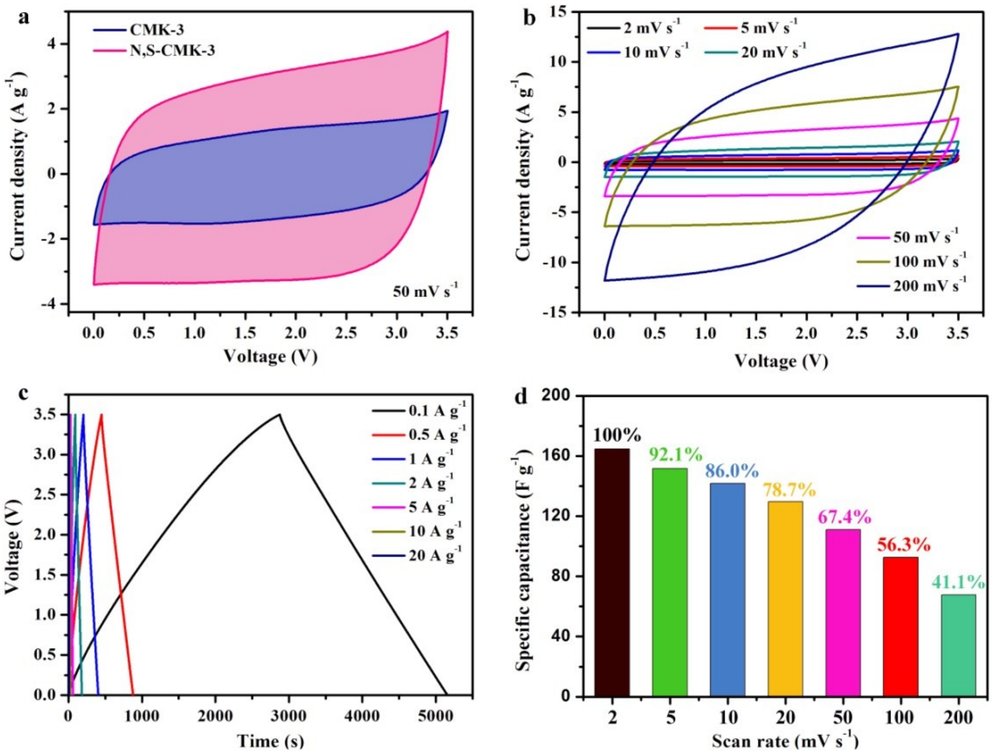

Figure S9. (a) CV curves of CMK-3 and N,S-CMK-3 electrodes at a scan rate of 50 mV s^{-1}. (b) CV curves of N,S-CMK-3 electrode at various scan rates ranging from 2 to 200 mV s^{-1}. (c) Galvanostatic charge-discharge curves at different current densities from 0.1 to 20 A g^{-1}. (d) specific capacitance values of N,S-CMK-3 calculated from CV curves at different scan rates.

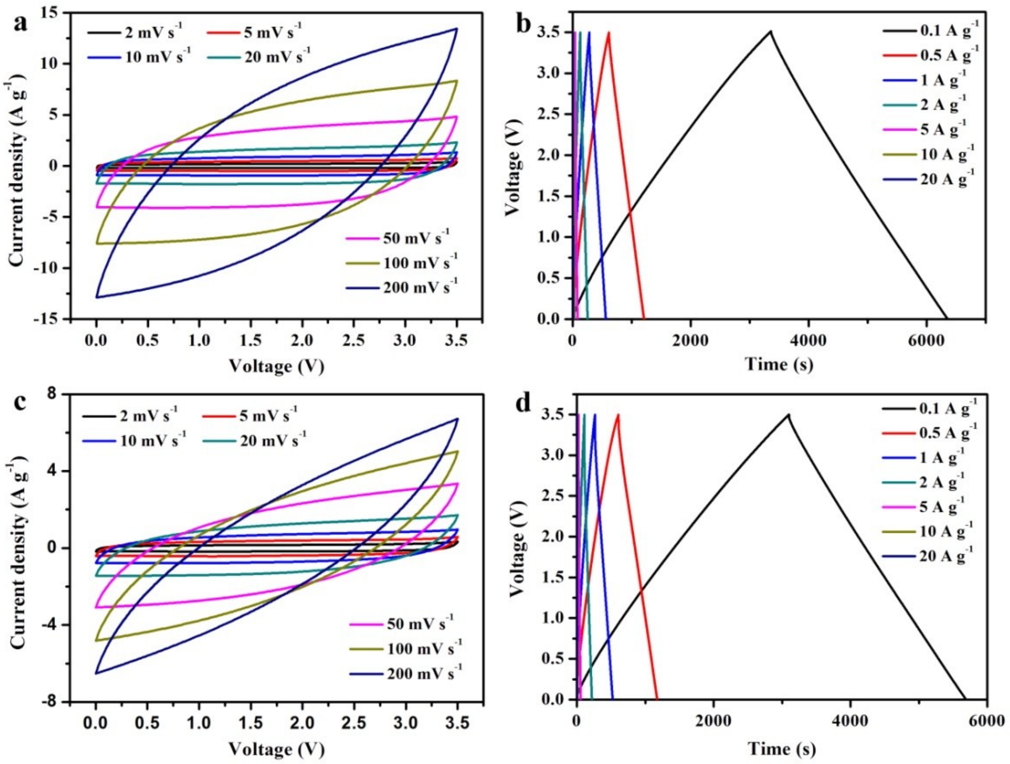

Figure S10. CV curves of (a) Fe-$NiCo_2S_4$@N,S-CMK-3 and (c) $NiCo_2S_4$@N,S-CMK-3 at various scan rates ranging from 2 to 200 mV s^{-1}. Galvanostatic charge-discharge curves of (b) Fe-$NiCo_2S_4$@N,S-CMK-3 and (d) $NiCo_2S_4$@N,S-CMK-3 at various current densities from 0.1 to 20 A g^{-1}.

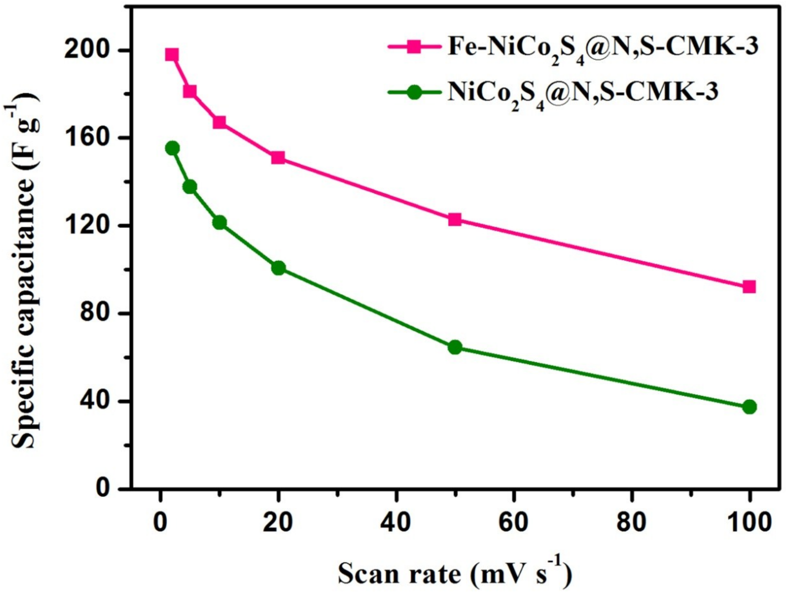

Figure S11. Plots of scan rates against the specific capacitance of Fe-NiCo$_2$S$_4$@N,S-CMK-3 and NiCo$_2$S$_4$@N,S-CMK-3.

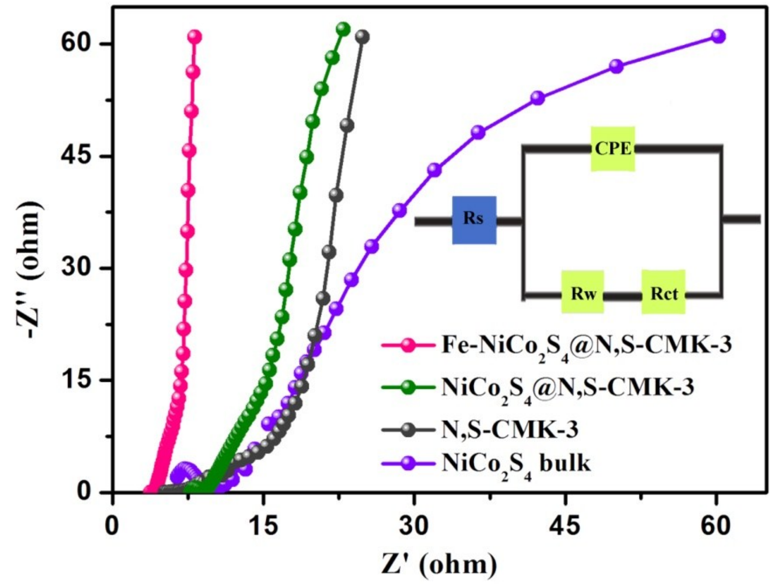

Figure S12. Nyquist plots of Fe-NiCo$_2$S$_4$@N,S-CMK-3, NiCo$_2$S$_4$@N,S-CMK-3, N,S-CMK-3, and NiCo$_2$S$_4$ bulk. Inset: equivalent circuit model (R_s, CPE, R_{ct}, and R_w denote the total ohmic resistance of electrodes, the capacitance of the double layer between electrode and electrolyte, electrochemical reaction impedance, diffusion of electroactive species, respectively).

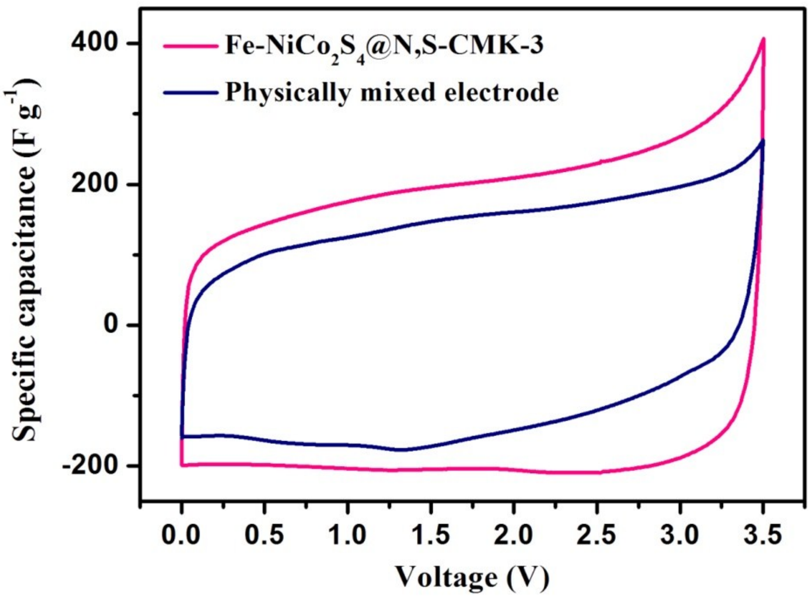

Figure S13. CV curves of Fe-$NiCo_2S_4$@N,S-CMK-3 electrode and physically mixed electrode of bulk Fe-$NiCo_2S_4$ and N,S-CMK-3 powders at a scan rate of 2 mV s^{-1}.

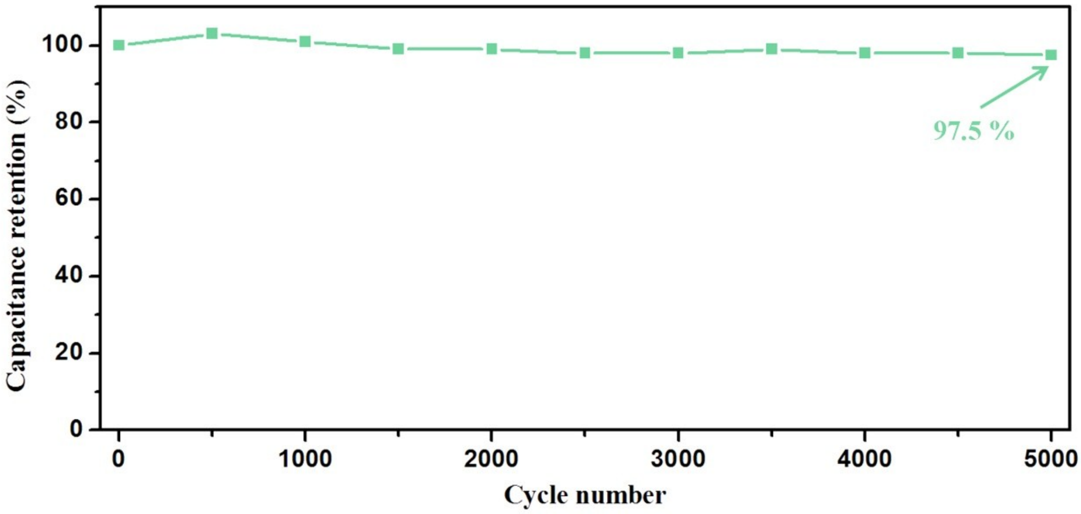

Figure S14. Cycling stability of Fe-$NiCo_2S_4$@N,S-CMK-3 at a constant current density of 5 A g^{-1}.

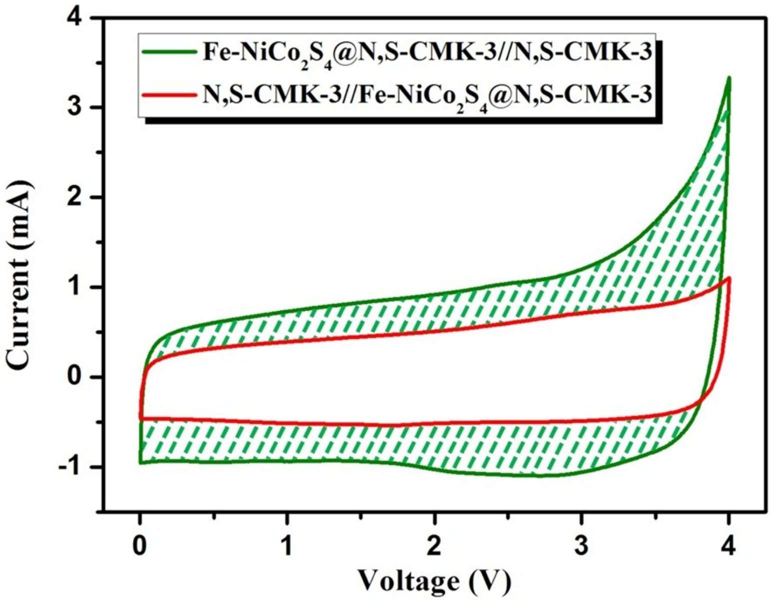

Figure S15. CV curves of Fe-NiCo$_2$S$_4$@N,S-CMK-3//N,S-CMK-3 and N,S-CMK-3//Fe-NiCo$_2$S$_4$@N,S-CMK-3 asymmetric supercapacitors at a scan rate of 2 mV s^{-1}. The left and right electrodes before and after "//" are positive and negative electrodes, respectively.

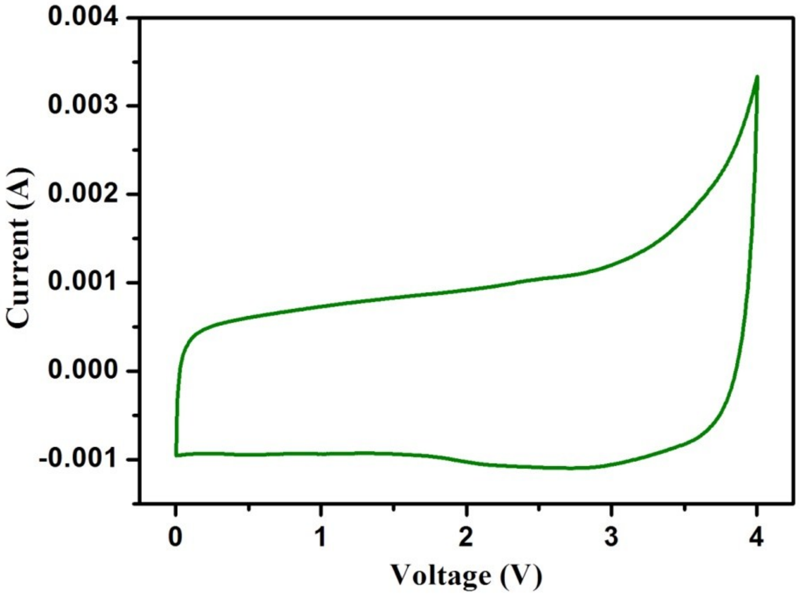

Figure S16. The CV curve for of Fe-NiCo$_2$S$_4$@N,S-CMK-3//N,S-CMK-3 asymmetric supercapacitor device at a low scan rate of 2 mV s^{-1}.

References:

[1] D. Y. Zhao, J. L. Feng, Q. S. Huo, N. Melosh, G. H. Fredrickson, B. F. Chmelka, G. D. Stucky, *Science* **1998**, *279*, 548-552.

[2] D. Y. Zhao, Q. S. Huo, J. L. Feng, B. F. Chmelka, G. D. Stucky, *J. Am. Chem. Soc.* **1998**, *120*, 6024-6036.

[3] K. S. Xia, Q. M. Gao, J. H. Jiang, J. Hu, *Carbon* **2008**, *46*, 1718-1726.

[4] F. L. Lai, J. R. Feng, R. Y. Yan, G. C. Wang, M. Antonietti, M. Oschatz, *Adv. Funct. Mater.* **2018**, *28*, 180129836.

[5] P. E. Blochl, *Phys. Rev. B* **1994**, *50*, 17953-17979.

[6] J. P. Perdew, K. Burke, M. Ernzerhof, *Phys. Rev. Lett.* **1996**, *77*, 3865-3868.

[7] H. J. Monkhorst, J. D. Pack, *Phys. Rev. B* **1976**, *13*, 5188-5192.